

First-principles study on *β*-GeS monolayer as high performance electrode material for alkali metal ion batteries

Meiqian Wan(万美茜), Zhongyong Zhang(张忠勇), Shangquan Zhao(赵尚泉), and Naigen Zhou(周耐根)
Citation: Chin. Phys. B, 2022, 31 (**9**): 096301. DOI: 10.1088/1674-1056/ac5d2e
Journal homepage: http://cpb.iphy.ac.cn; http://iopscience.iop.org/cpb

What follows is a list of articles you may be interested in

Evaluation of performance of machine learning methods in mining structure—property data of halide perovskite materials

Ruoting Zhao(赵若廷), Bangyu Xing(邢邦昱), Huimin Mu(穆慧敏), Yuhao Fu(付钰豪), and Lijun Zhang(张立军)
Chin. Phys. B, 2022, 31 (**5**): 056302. DOI: 10.1088/1674-1056/ac5d2d

Boron at tera-Pascal pressures

Peiju Hu(胡佩菊), Junhao Peng(彭俊豪), Xing Xie(谢兴), Minru Wen(文敏儒),Xin Zhang(张欣), Fugen Wu(吴福根), and Huafeng Dong(董华锋)
Chin. Phys. B, 2022, 31 (**3**): 036301. DOI: 10.1088/1674-1056/ac11e6

Two-dimensional MnN utilized as high-capacity anode for Li-ion batteries

Junping Hu(胡军平), Zhangyin Wang(王章寅), Genrui Zhang(张根瑞), Yu Liu(刘宇), Ning Liu(刘宁), Wei Li(李未), Jianwen Li(李健文), Chuying Ouyang(欧阳楚英), and Shengyuan A. Yang(杨声远)
Chin. Phys. B, 2021, 30 (**4**): 046302. DOI: 10.1088/1674-1056/abdda8

Effect of strain on electrochemical performance of Janus MoSSe monolayer anode material for Li-ion batteries: First-principles study

Guoqing Wang(王国庆), Wenjing Qin(秦文静), and Jing Shi(石晶)
Chin. Phys. B, 2021, 30 (**4**): 046301. DOI: 10.1088/1674-1056/abca24

First-principles study of the co-effect of carbon doping and oxygen vacancies in ZnO photocatalyst

Jia Shi(史佳), Lei Wang(王蕾), and Qiang Gu(顾强)
Chin. Phys. B, 2021, 30 (**2**): 026301. DOI: 10.1088/1674-1056/abc0db

---

First-principles study on β-GeS monolayer as high performance electrode material for alkali metal ion batteries

Meiqian Wan(万美茜), Zhongyong Zhang(张忠勇), Shangquan Zhao(赵尚泉)[†], and Naigen Zhou(周耐根)[‡]

School of Physics and Materials Science, Nanchang University, Nanchang 330031, *China*

(Received 27 December 2021; revised manuscript received 2 March 2022; accepted manuscript online 14 March 2022)

Based on the density functional theory calculations, we have investigated the feasibility of two-dimensional β-GeS monolayer as high-performance anodes for alkali metal ion batteries. The results show that the electrical conductivity of β-GeS monolayer can be enhanced after adsorbing the alkali metal atoms owing to the semiconductor-to-metal transition. The low diffusion barriers of alkali metal atoms on the β-GeS surface indicate a rapid charge/discharge rate without metal clustering. Moreover, the low average open-circuit voltage (0.211 V) and a high theoretical capacity (1024 mAh·g^{-1}) for Na suggest that the β-GeS monolayer is a promising anode material for Na-ion batteries with high performance.

Keywords: β-GeS, anode, alkali metal ion batteries, first-principles

PACS: 63.20.dk, 73.22.–f, 82.47.Cb, 96.15.Pf **DOI:** 10.1088/1674-1056/ac5d2e

1. Introduction

Lithium-ion batteries (LIBs) have achieved significant success among the alkali metal ion batteries (AMIBs), which are dominated the market of energy storage devices, such as portable electronic devices, electric vehicles, and grid-level energy storage.[1–3] However, the scarcity of lithium resources is difficult to meet the growing market demand, and the development of other alternative ion batteries has become an increasingly urgent need.[4–6] Sodium and potassium ion batteries (NIBs and KIBs) have entered the limelight as next-generation energy storage devices due to the abundant crustal resources of sodium and potassium elements and the similar working mechanism with LIBs.[7–10] Unexpectedly, the current LIBs commercial electrode graphite show poor storage capacity for NIBs and KIBs due to the energetic instability of the intercalated compounds with the larger radii Na and K. Hence, an important challenge for the successful commercial preparation of NIBs and KIBs is the lack of suitable anode materials with high capacity, rapid diffusion rate and good stability.

Recently, group-IV monochalcogenides, such as GeS, GeSe, SnS and SnSe, have attracted extensive attention due to their phosphorene-like layered structures with weak interlayer forces,[11–15] and in particular, bulk GeS has good potential as a LIBs anode material with high Li-ion storage capacity. Compared to bulk materials, two-dimensional (2D) materials, with large surface area, fast ion mobility and structural flexibility, are considered promising candidates for next-generation electrode materials to meet the higher performance demand.[16–30] Two-dimensional GeS monolayer has many different configurations, among which the orthogonal α-GeS structure (symmetry *Pcmn*) is the most widely studied. The α-GeS nanosheets were successfully prepared by liquid phase exfoliation in a custom sealed tip ultrasonic system, and subsequent analysis of the α-GeS nanosheet as anodes for LIBs revealed superb electrochemical performance, including high cycle stability of over 1000 cycles and high rate capability of over 10 A·g^{-1}.[31] However, theoretical studies showed that the capacity of 2D α-GeS as NIBs anode material could only reach 512 mAh·g^{-1}, which is slightly lower than that of C_2N (599.72 mAh·g^{-1}) and g-Mg_3N_2 (797 mAh·g^{-1}).[32–34] Note that previous studies show a suitable pore size and appropriate adsorption distance can effectively enhance the alkali metal (AM) adsorption capacity. Compared with α-GeS monolayer, the β-GeS (symmetry $Pmn2_1$) has bigger lattice constants and larger pore size, which may exhibit more excellent energy storage performance. Moreover, the binding energy of β-GeS and α-GeS are almost the same (the difference is less than 0.025 eV per atom), which suggests that the β-GeS monolayer may also have the same good stability as α-GeS.[35] However, most of the current researches on GeS nanosheet are mainly focused on the α-GeS monolayer, while little researches have been done on the β-GeS monolayer. The adsorption mechanism, diffusion energy barrier and theoretical capacity of β-GeS monolayer as the anode material of AMIBs are still unknown. At present, β-GeS has not been successfully prepared experimentally, but β-GeSe, which has the same crystal structure, stacking form and electronic properties as it, has been successfully synthesized recently.[36] With the rapid development of computer technology, theoretical calculations, an important tool in materials science research, can greatly help bridge some of the current experimental and technical gaps and aid in understanding the adsorption mechanisms of AM

[†]Corresponding author. E-mail: sqzhao@ncu.edu.cn
[‡]Corresponding author. E-mail: ngzhou@ncu.edu.cn

© 2022 Chinese Physical Society and IOP Publishing Ltd

atoms on novel battery materials. First-principles calculations dealing with the ground state of electrons in material systems can yield some electrochemical properties of electrode materials, such as adsorption energy, diffusion energy barrier, open-circuit voltage and theoretical capacity.[37]

In the present study, the performance of the β-GeS monolayer as the anode material for AMIBs have been systematically investigated by the first-principles calculations. The adsorption energy of AM atoms at different sites was calculated to identify the most stable adsorption site. The density of states analysis showed that the electrical conductivity of the β-GeS can be enhanced after adsorbing AM atoms due to the semiconductor-to-metal transition. Moreover, the β-GeS monolayer has a low diffusion energy barrier (0.258 eV), high theoretical capacity (1024 mAh·g^{-1}) and low operating voltage (0.211 V) for Na, suggesting that β-GeS monolayer can be used as an excellent high-performance anode material for NIBs.

2. Method

The theoretical calculations were adopted via the Vienna *ab initio* simulation package (VASP) based on the density functional theory. Projector augmented wave (PAW) was used to describe the interaction between the ionic real and outermost valence electrons.[38,39] The calculated cut-off energy was set to 520 eV. During the iterative process, the energy convergence threshold was 10^{-5} eV, and the force acting on each atom does not exceed 10^{-2} eV·Å^{-1}. The structure optimization and electron density of states calculations were performed by using the Monkhorst–Pack *k*-point grid settings, which were set to $4\times6\times1$ and $8\times12\times1$, respectively. The semi-empirical DFT-D3 method was employed for the correction of interlayer van der Waals forces.[40,41] The interlayer vacuum layer was set greater than 15 Å to prevent interlayer interaction forces. The phonon dispersion spectrum was calculated according to the finite displacement method in the Phonopy code to determine the dynamic stability. *Ab initio* molecular dynamics (AIMD) simulation was performed to confirm the thermal stability of the β-GeS monolayer. NVT ensemble was considered for the AIMD simulations with the Nosé–Hoover heat bath method.[42] The climbing image nudged elastic band (CI-NEB) method was used to study the minimum diffusion energy path of alkali metal atoms.[43,44] The atomic and electronic structures were analyzed by using the VESTA code.[45]

3. Results and discussion

3.1. Structure and stability of β-GeS monolayer

We construct the β-GeS monolayer with the space group $Pmn2_1$, and a unit cell contains two Ge atoms and two S atoms. After structural optimization, the calculated lattice constants of β-GeS monolayer are $a = 5.680$ Å and $b = 3.502$ Å, respectively, which are in good agreement with the previous theoretical results ($a = 5.68$ Å and $b = 3.51$ Å).[46] The β-GeS monolayer is an indirect bandgap semiconductor, and the bandgap calculated in this paper is 1.707 eV (Fig. S1), which is slightly smaller than the 1.77 eV in the Ref. [43]. These differences are because we used the DFT-D3 method instead of the DFT-D2 method in the Ref. [43], which can better describe the interactions between AM atoms and β-GeS monolayer with greater accuracy. The phonon spectrum of the β-GeS monolayer exists no negative imaginary frequency in the Brillouin zone, indicating the dynamic stability of the β-GeS monolayer (Fig. S2). A 3×3 supercell is adopted to examine the thermal stability of the β-GeS monolayer by performing AIMD simulations. The fluctuations of the total potential energy with simulation time are plotted in Fig. S3, where the total potential energy remains almost constant throughout the simulation period. The above results indicate that the β-GeS monolayer has good thermal stability.

The Fermi energy level can have an impact on the potential of as an electrode material.[47] Graphite has a high Fermi energy level (-4.31 eV) with low potential, which is suitable as a negative electrode material. The researchers were able to effectively modulate the electrochemical potential (2.7–3.7 V) by tuning the graphite derivative Fermi energy level (-8.36 to -8.47 eV) through a p-type doping strategy. The β-GeS monolayer has a higher Fermi energy level (-3.13 eV) and a narrower band gap, and the electrons introduced after the adsorption of AM atoms will fill in the higher energy level, resulting in a lower electrochemical potential. Thus, the β-GeS monolayer can exist in a relatively stable energy state and has promising potential as a low potential anode material.

3.2. Adsorption of AM atoms on β-GeS monolayer

To explore whether the β-GeS monolayer can be a suitable anode material for AMIBs, we firstly investigated the adsorption energy (E_{ad}) of a single AM atoms on the 2×2 β-GeS supercell. Considering the symmetry of the β-GeS monolayer structure, eight possible adsorption sites were chosen as shown in Fig. 1, which are the top of P–P triangle gravity center (C_1 and C_2 sites), the top of upper S-atom position (S_1 site), the top of lower S-atom position (S_2 site), the top of upper Ge-atom position (G_1 site), the top of lower Ge-atom position (G_2 site), and the top of hexagonal Ge–S rings center (H_1 and H_2 sites). The adsorption energy (E_{ad}) of an AM was calculated by the following formula:

$$E_{ad} = (E_{GeS-AM} - E_{GeS} - N\times E_{AM})/N, \tag{1}$$

where E_{GeS-AM} is the total energy of β-GeS after adsorbing AM atoms, E_{GeS} and E_{AM} are the total energies of GeS and

an AM atom in its bulk structure, respectively, N is the number of adsorbed AM atoms. After structural optimization, the AM atoms at C_1, G_2, H_1 and S_2 sites would spontaneously migrate to the adjacent C_2 site, and the AM atoms at G_1 and S_1 sites would finally migrate to the adjacent H_2 site. Only C_2 and H_2 sites are stable adsorption sites for AM atoms, and the corresponding adsorption energies are −0.223 eV and 0.273 eV (Li), −0.255 eV and 0.005 eV (Na), −0.678 eV and −0.465 eV (K), respectively. The adsorption energies of the H_2 site are positive for Li and Na atoms, indicating that these adsorption processes are non-spontaneous exothermic reactions. And the adsorption energy of the C_2 site and the H_2 site are both negative for the case of K atoms, while the C_2 site is more stable for the K atoms owing to the more negative adsorption energy. An interesting finding is that the E_{ad} values increase with the increase of the atomic radius, indicating stronger adsorption of β-GeS to heavier AM atoms. Thus, the C_2 site is the most stable adsorption site for Li, Na and K atoms, and the charge transfer and charge density distribution discussed later only consider the C_2 site adsorption conformations.

To further understand the adsorption mechanism, the differential charge density method has been used to analyze the charge distribution between AM atoms and the β-GeS monolayer, which is calculated by the following equation:

$$\Delta\rho = \rho_{\mathrm{GeS-AM}} - \rho_{\mathrm{GeS}} - \rho_{\mathrm{AM}}, \tag{2}$$

where ρ_{GeS} and $\rho_{\mathrm{GeS-AM}}$ are the charge density of the β-GeS before and after adsorb AM atoms, and ρ_{AM} is the charge density of isolated AM atoms. The differential charge density for AM atoms adsorption on the β-GeS monolayer is plotted in Fig. 2. There is a clear charge transfer between the AM atoms and the β-GeS monolayer, the charge depletion regions are mainly concentrated around the AM atoms, while the charge accumulation regions are mainly between the AM atoms and the β-GeS monolayer. Subsequently, the Bader charge analysis has been used to quantify the charge transfer of AM atoms, and the results show that Li, Na, and K atoms adsorbed on the β-GeS monolayer are contributed to 0.855, 0.800, and 0.821 electrons, respectively, and existed in the form of cations.

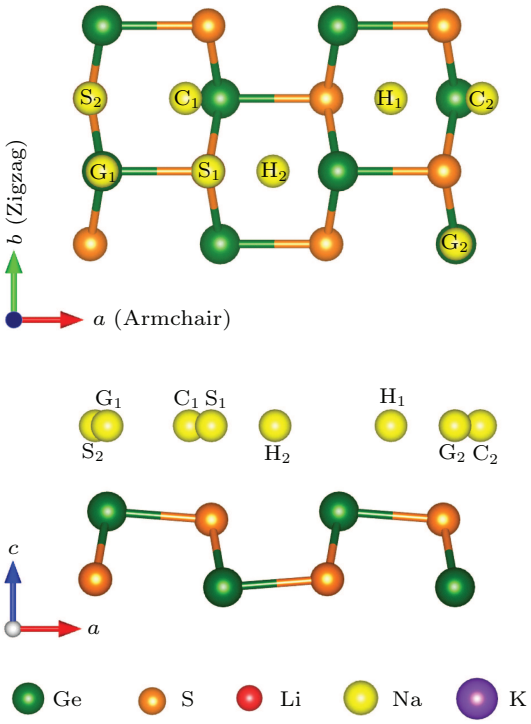


Fig. 1. Schematic diagram of eight highly symmetric adsorption sites on the surface of β-GeS monolayer, the yellow balls represent the possible sites of AM atoms.

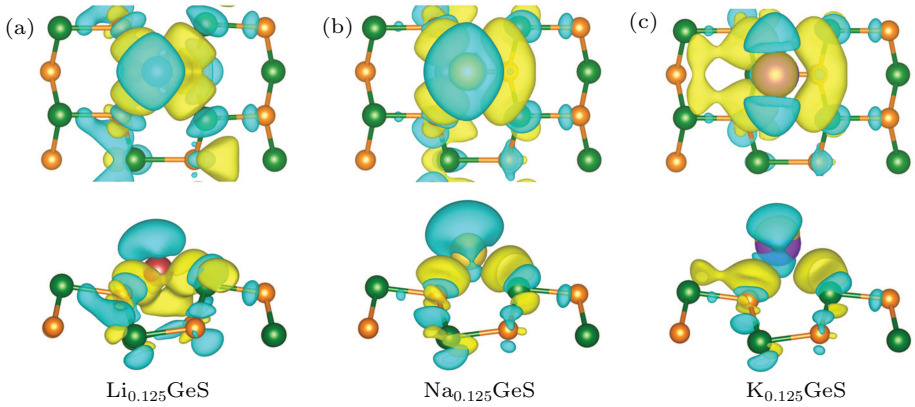


Fig. 2. The differential charge density distribution of β-GeS monolayer after adsorption of alkali metal atoms. (a) $Li_{0.125}GeS$, (b) $Na_{0.125}GeS$, (c) $K_{0.125}GeS$. The blue area represents electron depletion and the yellow area represents electron accumulation.

Meanwhile, the electronic density of states (DOS) of the β-GeS monolayer has been studied to identify how the electronic behavior changed. As shown in Fig. 3, the pristine β-GeS monolayer has no electronic state near the Fermi energy level and exhibits a semiconductor characteristic, which is consistent with the previous band structure calculation. However, the β-GeS systems after adsorb AM atoms exhibit metallic characteristics, the electrons near the Fermi energy level are

mainly provided by Ge atoms and the electrons of the valence band maximum (VBM) are mainly contributed by S atoms. The density composition of the conduction band minimum (CBM) and VBM electronic states are similar before and after the adsorption of AM atoms, and the main difference is that the Fermi energy level moves upwards and crosses the CBM.

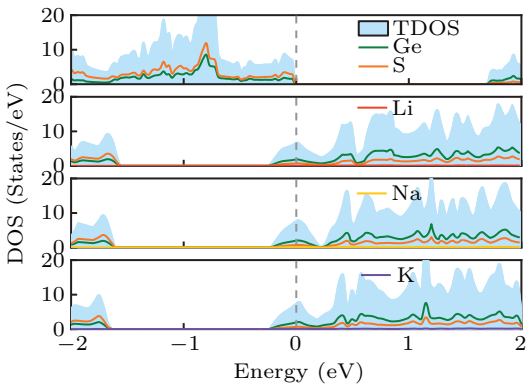


Fig. 3. DOS of (a) β-GeS, (b) $Li_{0.125}GeS$, (c) $Na_{0.125}GeS$, and (d) $Na_{0.125}GeS$.

This is because after the AM atoms are adsorbed on the β-GeS monolayer, the AM valence electrons are completely ionized into the conduction band, which increases the number of electrons in the conduction band and raises the Fermi energy level. All the above studies have shown that the adsorption of AM atoms on the β-GeS monolayer is accompanied by a large number of electrons transfer, which makes the Fermi energy level through the CBM and exhibits metallic properties. The semiconductor-to-metallic transition will enhance the electron conductivity, reduce the internal resistance during electron transfer and improve the overall performance of AMIBs.

3.3. Diffusion of AM atoms on the β-GeS monolayer

Fast charging is also a key technology for commercial batteries applications, which is determined by the diffusion barrier of AM atoms on the anode surface. Therefore, we have examined the diffusion of Li, Na, and K atoms on the β-GeS monolayer, and two diffusion paths are designed between two adjacent C_2 sites as shown in Fig. 4(a): zigzag direction (A→B) and armchair direction (B→C). The diffusion energy barriers are 0.914 eV (Li), 0.475 eV (Na) and 0.453 eV (K) along the armchair direction and 0.276 eV (Li), 0.258 eV (Na) and 0.208 eV (K) along the zigzag direction, respectively. Compared with Li atoms, the diffusion energy barriers of Na and K atoms are lower, this is because that as the radii of AM atoms increases, the larger the distance between the adsorption site and the β-GeS monolayer, the smaller the interaction force between the AM atoms and the β-GeS monolayer, and the easier for diffusion. The diffusion barriers are slightly lower or similar than other reported 2D electrode materials, such as GeP_3 (Li 0.5 eV, Na 0.27 eV and K 0.287 eV), MoN_2 (Li 0.78 eV, Na 0.56 eV and K 0.49 eV), SiC_3 (Li 0.47 eV, Na 0.34 eV and K 0.18 eV).[48–50]

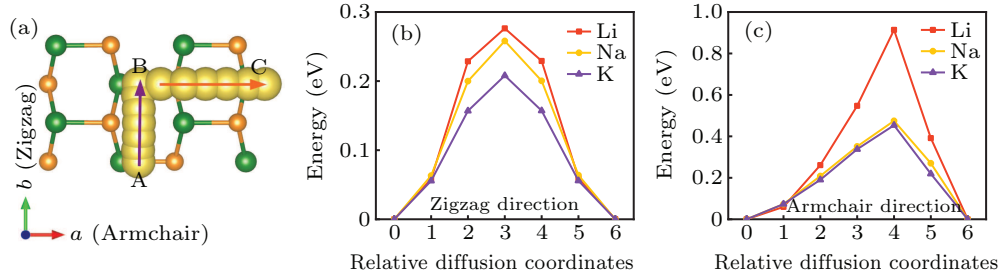


Fig. 4. (a) Schematic diagram of two diffusion paths on the β-GeS monolayer, (b) diffusion energy barrier curve of AM on the β-GeS monolayer surface along armchair direction, (c) diffusion energy barrier curve of AM on the β-GeS monolayer surface along the zigzag direction.

Considering the large difference in the diffusion energy barriers of alkali metal atoms along the armchair and zigzag directions (> 0.22 eV), this can impact the diffusion rate of AM atoms in different directions. The Arrhenius equation is used to quantify the difference in diffusion constants of AM atoms along the armchair and zigzag directions, and calculated as follows:

$$D \approx \exp(-E_a/k_B T), \tag{3}$$

where E_a and k_B are the diffusion barriers and Boltzmann's constant, respectively, and T is environmental temperature. According to the Arrhenius equation, the mobility of Li, Na and K along the zigzag direction are estimated about 5.2×10^{10}, 4.4×10^3, 1.360×10^4 times faster than that along armchair direction for β-GeS at the room temperature, respectively, showing a remarkable anisotropic diffusion feature. The β-GeS monolayer anode can easily achieve directional diffusion of AM atoms while preventing metal agglomeration. The low diffusion energy barrier and high diffusion constants of β-GeS monolayer make it a potentially excellent anode material for fast charge/discharge rates.

3.4. Theoretical voltage and specific capacity

The open-circuit voltage and theoretical capacity of β-GeS monolayer are futher discussed, because they have a decisive effect on the performance of AMIBs. The open-circuit

voltages (OCVs) of β-GeS monolayer at different adsorption concentrations of AM atoms under the neglect of volume and entropy can be calculated by the following equation:

$$V = -\frac{E_{(\mathrm{AM}_{x_2}\mathrm{GeS})} - E_{(\mathrm{AM}_{x_1}\mathrm{GeS})} - (x_2 - x_1)E_{\mathrm{AM}}}{(x_2 - x_1)ne}, \quad (4)$$

where $E_{(\mathrm{AM}_{x_2}\mathrm{GeS})}$ and $E_{(\mathrm{AM}_{x_1}\mathrm{GeS})}$ denote the total energy of the system for β-GeS monolayer adsorption concentrations of x_2 and x_1, respectively. n is the number of AM valence electrons and e is the unit charge. As a suitable anode material, the open circuit voltage should be in the range of 0–1.0 V. Below 0 V will cause a dendritic phenomenon, while above 1.0 V will bring a lower operating voltage of batteries. The open circuit voltage curves and the corresponding optimized structures for different adsorption concentrations of AM atoms are shown in Figs. 5(a)–5(c). The adsorption of Li atoms prefers unilateral adsorption, the adsorbed atoms are all located on the same side of the β-GeS monolayer, and the corresponding stoichiometric ratio at the maximum adsorption capacity is $Li_{0.5}GeS$. When the adsorption stoichiometry ratio exceeds $Li_{0.5}GeS$, the strong interaction between Li atoms and β-GeS monolayers produces severe structural distortion and the Ge–S bond breaks to form Li–S bonds, leading to irreversible destruction of the β-GeS structure. A similar phenomenon that Ge–Se bond breaks to form Li–Se bonds was observed in the lithiation of GeSe monolayer.[51] Therefore, it means that the β-GeS monolayer is unsuitable for LIBs anode. As for the Na and K atoms adsorption, the adsorbed atoms prefer simultaneous adsorption on the upper and lower surfaces, and the stoichiometric ratios of the maximum adsorption amounts are Na_4GeS and KGeS, respectively. Meanwhile, the β-GeS has the open-circuit voltage in the ranges are 0.297–0.382 V, 0.293–0.177 V, and 0.674–0.168 V for of Li, Na, and K with the corresponding average OCVs of 0.340 V, 0.211 V, and 0.400 V. These average OCVs values are between those of conventional anode materials (e.g., graphite 0.11 V and TiO_2 1.5–1.8 V), and lower than those 2D anode materials such as h-BAs (Li 0.49 V, Na 0.35 V and 0.26 V), and FeSe (Li 0.88 V, Na 0.49 V and 0.38 V).[52–55] The average OCVs of Li, Na and K are in the ideal voltage range of 0.00–1.00 V for the β-GeS monolayer.

The maximum theoretical capacities (C) of AM atoms can be calculated by

$$C = \frac{x_{\max} nF}{M_{\mathrm{GeS}}}, \quad (5)$$

where $x_{\max}$ is the maximum ratio of adsorbed AM atoms, F is the Faraday constant (26.8 Ah·mol^{-1}) and M_{GeS} is the atomic mass of GeS (104.7 g·mol^{-1}).

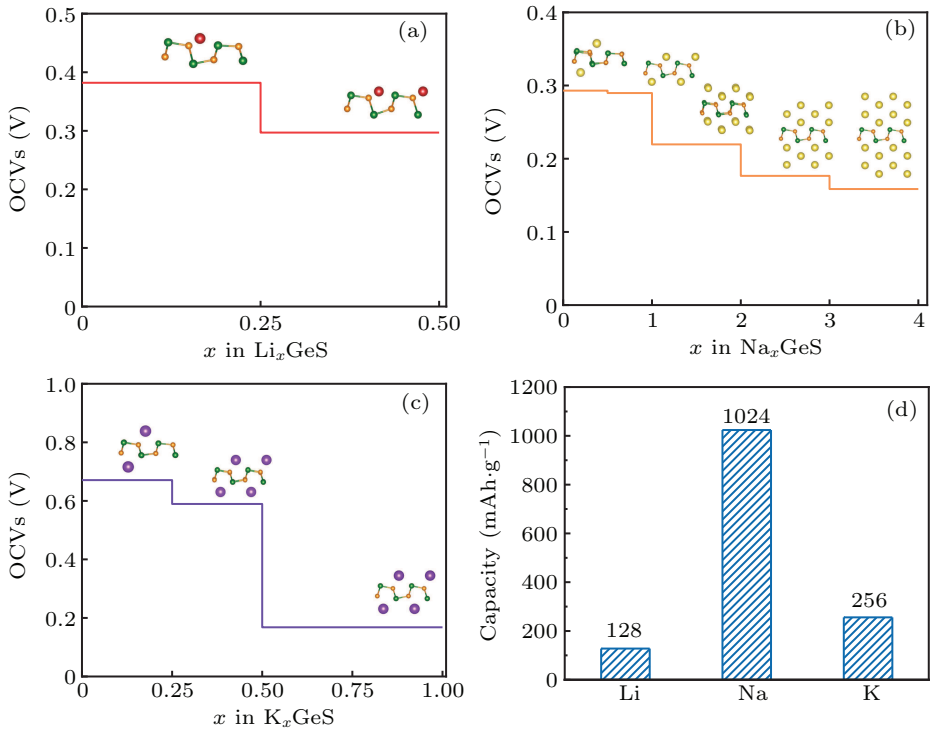


Fig. 5. OVCs of β-GeS monolayer during the intercalation of AM atoms, (a) Li_xGeS, (b) Na_xGeS, (c) K_xGeS. (d) The theoretical capacities of AM atoms on the β-GeS monolayer.

The specific capacity (Fig. 5(d)) of the 2D β-GeS anodes for Li, Na and K atoms are 128 mAh·g^{-1}, 1024 mAh·g^{-1}, 256 mAh·g^{-1}, respectively. The β-GeS monolayer is not suitable as the anode of Li-ion battery because of low Li storage capacity and poor stability. While, for Na and K atoms, the theoretical capacities are slightly higher than

those reported for some 2D materials, such as MXenes (Na <400 mAh·g^{-1} and K < 200 mAh·g^{-1}), Mo_2C (Na 132 mAh·g^{-1} and K 65 mAh·g^{-1}), MoS_2 (Na 670 mAh·g^{-1}), α-GeS (Na 512 mAh·g^{-1} and K 256 mAh·g^{-1}) and graphite (Na 35 mAh·g^{-1} and K 279 mAh·g^{-1}).[32,56–61] The sodium storage capacity of β-GeS monolayer is twice of that of α-GeS, which is due to the larger lattice constant and larger pore size of β-GeS, the distance between adsorbed atoms is larger, and the repulsive force generated between Na ions will be weakened, which is more favorable to Na atom adsorption. However, the effect of pore size on the K atoms adsorption is not significant, the adsorption energy is smaller for the second layer of K atoms due to the large radius of K atoms and the long distance between K and β-GeS. As shown in Table 1, like other Ge-based chalcogenides, the β-GeS monolayer is more suitable as electrode material for NIBs with high theoretical capacity.

Table 1. The specific capacities and energy barriers of different 2D anode materials for AM ion batteries.

	Capacity (mAh·g^{-1})			Energy barrier (eV)			Reference
	Li	Na	K	Li	Na	K	
β-GeS	128	1024	256	0.276	0.258	0.208	this work
α-GeS	256	512	256	0.236	0.090	0.050	[32]
β-GeSe		353.65	353.65	0.08	0.052		[62]
α-GeSe	176.78	707.12	530.44	0.291	0.115	0.11	[49]
Cr_2CO_2	331	276	239	0.12	0.09	0.04	[63]
Ti_3C_2	447.8	351.8	191.8	0.068	0.096	0.103	[26]

Moreover, the electron localization functions (ELF) of Na_4GeS and KGeS are displayed in Fig. 6, where the value of 0.00 indicates no charge density distribution, while the values of 0.50 and 1.00 indicate fully delocalized and fully localized electrons. For Na_4GeS and KGeS, the electrons form a negative electron cloud (NEC) around the Na and K atoms, which can shield the repulsive forces between metal cations and avoid the occurrence of clusters, thus better maintaining the stability of the adsorption system. Compared with current commercial graphite electrodes, β-GeS monolayer has high capacity, low diffusion energy barrier and low open-circuit voltage as anode material for NIBs. From the above described findings, we conclude that β-GeS monolayers can be considered as excellent anode materials for NIBs.

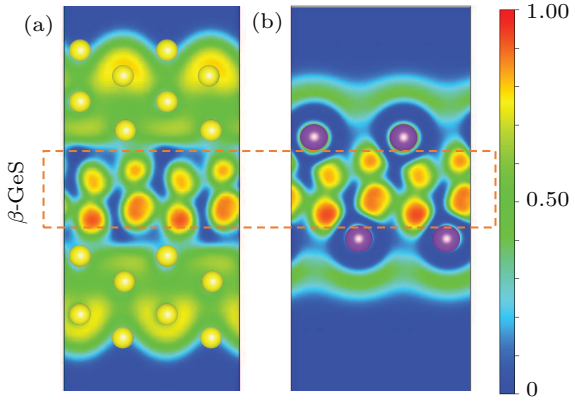


Fig. 6. ELF maps sliced in (010) direction of (a) Na_4GeS and (b) KGeS.

4. Conclusion

We have systematically investigated the performance of β-GeS as anode material for AMIBs using the first-principles calculations. The electrical conductivity of β-GeS can be enhanced after the adsorption of AM atoms due to the semiconductor-to-metal transition. In addition, the low diffusion energy barrier of AM atoms on the β-GeS monolayer provides a rapid charge/discharge rate for AIMBs applications. Moreover, we found the β-GeS monolayer with larger pores has twice Na storage capacity (1024 mAh·g^{-1}) than that of α-GeS. Considering the low diffusion barrier (0.258 eV), high capacity and low average OCV (0.211 V) for Na, the β-GeS monolayer can be used as a high performance NIBs anode material.

Acknowledgements

Project supported by the the National Natural Science Foundation of China (Grant Nos. 52062035 and 51861023) and the Major Discipline Academic and Technical Leaders Training Program of Jiangxi Province, China (Grant No. 20213BCJ22056).

References

[1] Dunn B, Kamath H and Tarascon J M 2011 *Science* **334** 928
[2] Lin D C, Liu Y Y and Cui Y 2017 *Nat. Nanotechnol.* **12** 194
[3] Hu J, Wang Z, Zhang G, Liu Y, Liu N, Li W, Li J, Ouyang C and Yang S A 2021 *Chin. Phys. B* **30** 046302
[4] Wang L, Huang Z, Wang B, Liu G, Cheng M, Yuan Y, Luo H, Gao T, Wang D and Shahbazian-Yassar R 2019 *ACS Appl. Mater. Inter.* **11** 10663
[5] Fan X, Zheng W T and Kuo J L 2012 *ACS Appl Mater. Inter.* **4** 2432
[6] Li J, Yan S, Wu W X, Li L X, Li. H D and Hashem S 2020 *Comput. Theor. Chem.* **1181** 112796
[7] Zhou C, Huang J and Duan X 2021 *Chin. Phys. B* **30** 056801
[8] Zhao Z, Yu T, Zhang S, Xu H, Yang G and Liu Y 2019 *J. Mater. Chem. A* **7** 405
[9] Zhang W, Mao J, Li S, Chen Z and Guo Z 2017 *J. Am. Chem. Soc.* **139** 3316
[10] Hu Y, Wang J and Lin H 2021 *Colloid Surf. A* **619** 126536

[11] Cho Y J, Im S H, Kim H S, Myung Y, Back S H, Lim Y R, Jung C S, Jang D M, Park J, Cha E H, Cho W I, Shojaei F and Kang H S 2013 *Acs Nano* **7** 9075
[12] Sung G K and Park C M 2017 *J. Mater. Chem. A* **5** 5685
[13] Zhou X, Hu X Z, Jin B, Yu J, Liu K L, Li H Q and Zhai T Y 2018 *Adv. Sci.* **5** 1800478
[14] Chaki S H, Chaudhary M D and Deshpande M P 2015 *J. Therm. Anal. Calorim.* **120** 1261
[15] Shi X L, Tao X Y, Zou J and Chen Z G 2020 *Adv. Sci.* **7** 1902923
[16] Berdiyorov G R 2015 *Appl. Surf. Sci.* **359** 153
[17] Wang G, Qin W and Shi J 2021 *Chin. Phys. B* **30** 046301
[18] Hassan A S, Moyer K, Ramachandran B R and Wick C D 2016 *J. Phys. Chem. C* **120** 2036
[19] Jing Y, Zhou Z, Cabrera C R and Chen Z F 2013 *J. Phys. Chem. C* **117** 25409
[20] Shi L and Zhao T 2017 *J. Mater. Chem. A* **5** 3735
[21] Khantha M, Cordero N A, Molina L M, Alonso J A and Girifalco L A 2004 *Phys. Rev. B* **70** 125422
[22] Tan X, Li F and Chen Z 2014 *J. Phys. Chem. C* **118** 25825
[23] Mortazavi M, Wang C, Deng J, Shenoy V B and Medhekar N V 2014 *J. Power. Sources* **268** 279
[24] Wu J, Wang D, Liu H, Lau W M and Liu L M 2015 *Rsc Adv.* **5** 21455
[25] Wang Y, Song N, Song X, Zhang T, Zhang Q and Li M 2018 *Rsc Adv.* **8** 10848
[26] Tang Q, Zhou Z and Shen P W 2012 *J. Am. Chem. Soc.* **134** 16909
[27] Tang X, Guo X, Wu W J and Wang G X 2018 *Adv. Energ. Mater.* **8** 1801897
[28] Kulish V V, Malyi O I, Persson C and Wu P 2015 *Phys. Chem. Chem. Phys.* **17** 13921
[29] Chowdhury C, Karmakar S and Datta A 2016 *Acs Energy Lett.* **1** 253
[30] Banerjee S, Periyasamy G and Pati S K 2014 *J. Mater. Chem. A* **2** 3856
[31] Lam D, Chen K S, Kang J, Liu X and Hersam M C 2018 *Chem. Mater.* **30** 2245
[32] Li F, Qu Y and Zhao M 2016 *J. Mater. Chem. A* **4** 8905
[33] Ding Y, Deng Q, You C, Xu Y, Li J and Xiao B 2020 *Phys. Chem. Chem. Phys.* **22** 21208
[34] Xiong L, Wang H, Xiong W, Yu S and Ouyang C 2019 *Rsc Adv.* **9** 27378
[35] Hu T and Dong J M 2016 *Phys. Chem. Chem. Phys.* **18** 32514
[36] Rohr F O, Ji H, Cevallos F A, Gao T, Ong N P and Cava R J 2017 *J. Am. Chem. Soc.* **139** 2771
[37] Shi S, Gao J, Liu Y, Zhao Y, Wu Q, Ju W, Ouyang C and Xiao R 2016 *Chin. Phys. B* **25** 018212
[38] Blochl P E 1994 *Phys. Rev. B Condens. Matter.* **50** 17953
[39] Perdew J P, Burke K and Ernzerhof M 1998 *Phys. Rev. Lett.* **77** 3865
[40] Grimme S, Antony J, Ehrlich S and Krieg H 2010 *J. Chem. Phys.* **132** 154104
[41] Grimme S, Ehrlich S and Goerigk L 2011 *J. Comput. Chem.* **32** 1456
[42] Liu B, Gao T, Liao P, Wen Y, Yao M, Shi S and Zhang W 2021 *Phys. Chem. Chem. Phys.* **23** 18784
[43] Nose S 1984 *J. Chem. Phys.* **81** 511
[44] Henkelman G, Uberuaga B P and Jonsson H 2000 *J. Chem. Phys.* **113** 9901
[45] Momma K and Izumi F 2011 *J. Appl. Crystall.* **44** 1272
[46] Yin H, Liu C, Zheng G P, Wang Y and Ren F 2019 *Appl. Phys. Lett.* **114** 192903
[47] Wang Z, Wang D, Zou Z, Song T, Ni D, Li Z, Shao X, Yin W, Wang Y, Luo W, Wu M, Avdeev M, Xu B, Shi S, Ouyang C and Chen L 2020 *Natl. Sci. Rev.* **7** 1768
[48] Deng X, Chen X, Huang Y, Xiao B and Du H 2019 *J. Phys. Chem. C* **123** 4721
[49] Zhang X, Yu Z, Wang S S, Guan S, Yang H Y, Yao Y and Yang S A 2016 *J. Mater. Chem. A* **4** 15224
[50] Wang Y and Li Y 2020 *J. Mater. Chem. A* **8** 4274
[51] Sannyal A, Zhang Z, Gao X and Jang J 2018 *Comp. Mater. Sci.* **154** 204
[52] Persson K, Hinuma Y, Meng Y S, Van der Ven A and Ceder G 2010 *Phys. Rev. B* **82** 125416
[53] Yang Z G, Choi D, Kerisit S, Rosso K M, Wang D H, Zhang J, Graff G and Liu J 2009 *J. Power Sources* **192** 588
[54] Khossossi N, Banerjee A, Benhouria Y, Essaoudi I, Ainane A and Ahuja R 2019 *Phys. Chem. Chem. Phys.* **21** 18328
[55] Lv X, Li F, Gong J, GuJ, Lin S and Chen Z 2020 *Phys. Chem. Chem. Phys.* **22** 8902
[56] Yu X, Dall'Agnese Y, Naguib M, Gogotsi Y and Kent P 2014 *Acs Nano* **8** 9606
[57] Aslam M K, Niu Y B and Xu M W 2021 *Adv Energy Mater.* **11** 2000681
[58] Bak S M Q, Yang R M, Lee W L, Yu S, Anasori X Q, Lee B, Gogotsi H and Yang X Q 2017 *Adv Energy Mater.* **7** 1700959
[59] Chen J F, Hu Q K, Zhou A G and Sun D D 2015 *Acta Phys.-Chim. Sin.* **31** 2278
[60] Mortazavi M, Wang C, Deng J, Shenoy V B and Medhekar N V 2014 *J. Power Sources* **268** 279
[61] Sun Q, Dai Y, Ma Y, Jing T, Wei W and Huang B 2016 *J. Phys. Chem. Lett.* **7** 937
[62] Zhou Y, Zhao M, Chen Z W, Shi X M and Jiang Q 2018 *Phys. Chem. Chem. Phys.* **20** 30290
[63] Li F Y, Cabrera C R, Wang J Y and Chen Z F 2016 *Rsc Adv.* **6** 81591